

A Pressure-Based Diffusion Model for Influence Maximization on Social Networks

Curt Stutsman¹, Eliot W. Robson¹, Abhishek K. Umrawal¹

¹University of Illinois Urbana-Champaign
Urbana, Illinois 61801 USA

curtiss8@illinois.edu, erobson2@illinois.edu, aumrawal@illinois.edu

Abstract

In many real-world scenarios, an individual’s local social network carries significant influence over the opinions they form and subsequently propagate. In this paper, we propose a novel diffusion model — **the Pressure Threshold model (PT)** — for dynamically simulating the spread of influence through a social network. This model extends the popular Linear Threshold (LT) model by adjusting a node’s outgoing influence in proportion to the influence it receives from its activated neighbors. We examine the Influence Maximization (IM) problem under this framework, which involves selecting seed nodes that yield maximal graph coverage after a diffusion process, and describe how the problem manifests under the PT model. Experiments on real-world networks, supported by enhancements to the open-source network-diffusion library CyNetDiff, reveal that the PT model identifies seed sets distinct from those chosen by LT. Furthermore, the analyses show that densely connected networks amplify pressure effects far more strongly than sparse networks.

1 Introduction

1.1 Motivation

Diffusion processes within human populations aim to imitate how behaviors, information, diseases, and more propagate through social networks. Diffusion models provide the underlying mathematics that dictate how attributes spread from one node to the next. Early diffusion models provided critical insights into these processes, paving the way for numerous practical applications in epidemiology and the social sciences. With the advent of digital platforms and the increasing significance of viral marketing around the turn of the twenty-first century (Evans and McKee 2010), diffusion models became crucial for solving the Influence Maximization (IM) problem, first formulated by Domingos and Richardson (Domingos and Richardson 2001). The goal of the IM problem is to select a set of k seed nodes in a network such that the expected spread of influence is maximized after a diffusion process. The choice of diffusion model significantly impacts how influence propagates, thus determining the effectiveness of seed node selection.

Copyright © 2026, Stutsman, Robson, and Umrawal. This work is licensed under a Creative Commons Attribution-NoDerivatives 4.0 International License.

The IM problem was popularized by Kempe et al. (Kempe, Kleinberg, and Tardos 2003a), who proposed basic greedy algorithms for solving the problem. Kempe et al. also gave the first formal definitions for the Linear Threshold (LT) and Independent Cascade (IC) diffusion models, which remain the most commonly used models in research today. These models seek to not only mathematically define the propagation of influence but also accurately represent genuine human interactions in real-world communities. However, despite their utility, traditional models often inadequately capture significant interpersonal phenomena such as reinforcement effects within echo chambers, where repeated exposure to an idea intensifies existing beliefs and behaviors (Bakshy, Messing, and Adamic 2015). A growing body of empirical work shows that online diffusion is shaped by local reinforcement: false or novel items can spread farther, faster, and deeper than truth on Twitter (Vosoughi, Roy, and Aral 2018), users self-organize into homophilic clusters that bias transmission toward like-minded peers (Cinelli et al. 2021; Brugnoli et al. 2019), and adoption probabilities often rise with multiple confirming exposures, i.e., complex contagion (Mønsted et al. 2017).

To address these shortcomings and better represent realistic social dynamics, this research introduces the Pressure Threshold model (PT), an extension of the LT model. The PT model introduces dynamic feedback mechanisms, wherein nodes amplify their outgoing influence proportional to the incoming influence from activated neighbors. This mechanism directly operationalizes the empirically observed reinforcement pattern: when a node activates under substantial ‘pressure,’ it becomes a stronger advocate in subsequent steps, thereby capturing within-community amplification consistent with observed diffusion regularities (Vosoughi, Roy, and Aral 2018; Cinelli et al. 2021). Such reinforcement reflects realistic social scenarios. For example, individuals are more likely to strongly advocate a product when many of their friends or peers have already adopted it (Gunawan, Rahmania, and Kenang 2023). By making this feedback explicit while retaining LT’s additive semantics, PT offers a simple and interpretable way to model reinforcement beyond static LT/IC assumptions, aligning the diffusion mechanism with documented online behaviors and providing new leverage for IM analyses.

1.2 Literature Review

Diffusion models have a long history of use, extending beyond the IM problem. We now review the history of diffusion models, their role in Influence Maximization, and dynamic approaches related to the Pressure Threshold model.

Early Diffusion Models: The study of diffusion models originated in epidemiology and sociology. Early foundational work by Kermack and McKendrick (1927) introduced the Susceptible-Infected-Recovered (SIR) epidemiological model, setting the stage for understanding contagion processes (Kermack and McKendrick 1927). In social networks, Granovetter’s threshold model (1978) became foundational, conceptualizing adoption based on cumulative peer influence (Granovetter 1978). Both the Linear Threshold (LT) and Independent Cascade (IC) models were later formalized by Kempe et al. (Kempe, Kleinberg, and Tardos 2003a), and remain standard in IM research. These models provide the basis for most algorithmic work on influence spread.

Influence Maximization: The IM problem was explicitly formulated by Domingos and Richardson in the context of viral marketing, aiming to maximize influence spread through optimal seed selection (Domingos and Richardson 2001). Kempe et al. advanced IM research by proving NP-hardness and introducing greedy algorithms with approximation guarantees (Kempe, Kleinberg, and Tardos 2003a), sparking extensive follow-up work.

Improvements to IM: Subsequent research refined IM algorithms for scalability and efficiency. Leskovec et al. introduced CELF, reducing complexity while preserving guarantees (Leskovec et al. 2007a), later improved by CELF++ (Goyal, Lu, and Lakshmanan 2011). Borgs et al. developed Reverse Influence Sampling (RIS) for near-optimal scalability (Borgs et al. 2014). Chen et al. proposed the degree discount heuristic for faster, though less optimal, solutions (Chen, Wang, and Yang 2009). Recent work explores community-aware heuristics (Umrawal and Aggarwal 2023) and learning-based approaches (Kumar et al. 2022). Beyond the original problem, variants include partial incentives (Chen, Wu, and Yu 2020; Umrawal, Aggarwal, and Quinn 2023; Bhimaraju et al. 2024), online settings (Agarwal et al. 2022; Nie et al. 2022), fairness (Becker et al. 2022; Lin et al. 2023; Nguyen et al. 2022), and deep learning methods (Kumar et al. 2022). See (Li et al. 2023) for a detailed survey.

Dynamic Diffusion Models: Unlike static LT and IC models, dynamic models capture evolving network structures and influence weights. Zhuang et al. addressed edge dynamics over time (Zhuang et al. 2013). Xie et al. proposed *DynaDiffuse*, combining continuous-time propagation with dynamic edge weights (Xie et al. 2015). These approaches share conceptual similarities with PT, which introduces adaptive influence updates.

Predictive Comparison of Diffusion Models: Some studies compare diffusion models against real-world cascades. Kuo et al. evaluated predictive accuracy, finding IC superior for direct prediction tasks, while LT performed better in indirect comparisons (Kuo et al. 2011). Ananthasubra-

maniam et al. analyzed Twitter hashtag propagation, showing accuracy depends on network topology and content type (Ananthasubramaniam et al. 2024). Aral and Walker validated cumulative influence in product adoption, supporting threshold-based assumptions (Aral and Walker 2012).

Shortcomings of Existing Models: Despite progress, existing models often overlook reinforcement dynamics evident in online networks and misinformation cascades. Bakshy et al. showed ideological reinforcement and echo chambers amplify diffusion on Facebook (Bakshy, Messing, and Adamic 2015). Vosoughi et al. demonstrated that false news spreads faster and deeper than truth, driven by repeated exposure and amplification (Vosoughi, Roy, and Aral 2018). Such findings underscore the need for models that incorporate local reinforcement, a gap addressed by the Pressure Threshold model.

In summary, while prior work has advanced IM theory and algorithms, gaps remain in modeling dynamic feedback and empirically observed reinforcement. Our research bridges these gaps by introducing a diffusion model that explicitly accounts for local social reinforcement, supported by empirical evidence.

1.3 Contribution

This paper makes four primary contributions:

1. **Pressure Threshold (PT) Model.** We introduce the Pressure Threshold diffusion model, an extension of the Linear Threshold (LT) model that incorporates local reinforcement: when a node activates, it increases its outgoing influence in proportion to the cumulative incoming pressure that triggered its activation. This mechanism captures empirically observed amplification within communities while preserving the additive semantics of LT.
2. **Theoretical Properties.** We prove that influence maximization under PT is NP-hard (by reduction from LT) and establish that PT preserves monotonicity. We also show by counterexample that PT is not submodular when the amplification parameter $\alpha > 0$, clarifying the scope of classical greedy-approximation guarantees.
3. **Implementation.** We enhance the CyNetDiff (Robson, Reddy, and Umrawal 2024) Python library for accelerated simulations, leveraging Cython-based kernels to support large-scale Monte Carlo evaluation across diffusion models, including PT. These improvements enable practical experiments on real-world graphs at scale.
4. **Empirical Analysis.** Across real and synthetic networks, PT (i) produces seed sets distinct from LT and (ii) often achieves larger final spreads for comparable budgets. Although submodularity does not hold in general, we observe approximate submodular behavior in large networks for small α , under which greedy strategies remain effective. Analyses on synthetic topologies highlight regimes where PT’s reinforcement is especially beneficial (e.g., denser structures with more opportunities for amplification).

Collectively, these results indicate that explicitly modeling local reinforcement yields diffusion dynamics and seed-

selection behavior that are not captured by static LT/IC formulations, while remaining computationally tractable for influence maximization workflows.

1.4 Organization

The remainder of the paper is organized as follows. Section 2 introduces preliminaries and formally defines the Pressure Threshold model, including the NP-hardness argument. Section 3 provides a small-scale walk-through of PT dynamics and presents our analysis of monotonicity and non-submodularity, including a counterexample. Section 4 describes our experimental setup, implementation details (CyNetDiff), datasets, and results on both real-world and synthetic networks. Section 5 concludes with implications, limitations, and avenues for future work.

2 Preliminaries and Model Formulation

In this section, we formally establish foundational concepts and clearly define the Pressure Threshold model (PT). We discuss existing diffusion models, formalize the proposed PT model, and analyze its computational complexity.

2.1 Linear Threshold Model and Influence Maximization

Diffusion models mathematically describe how information, ideas, behaviors, or diseases propagate through a network. Two of the most widely studied models in the context of influence maximization are the Linear Threshold (LT) model and the Independent Cascade (IC) model, formalized by Kempe et al. (Kempe, Kleinberg, and Tardos 2003a).

Given that the PT model is a generalization of the LT model, we will now give a formal definition of the LT model. Let $G = (V, E)$ be a directed graph where V is the set of nodes and $E \subseteq V \times V$ is the set of edges. Each edge $(u, v) \in E$ is assigned a weight $w_{uv} \in [0, 1]$ such that for each node v , $\sum_{u \in N(v)} w_{uv} \leq 1$, where $N(v)$ denotes the in-neighbors of v . The edge weight is meant to quantify the degree to which node u can influence node v . Additionally, each node v has a threshold θ_v drawn uniformly at random from the interval $(0, 1]$. Initially, a set of seed nodes $S \subseteq V$ is activated. In each subsequent discrete time step, an inactive node v becomes active if the total weight of its active in-neighbors meets or exceeds its threshold:

$$\sum_{u \in P(v)} w_{uv} \geq \theta_v,$$

where $P(v) = \{u \in A_t : (u, v) \in E\}$ denotes the set of active parent nodes (or in-neighbors) of v . This process continues until no new nodes can be activated, and the diffusion ceases. For clarity, we consistently use $N(v)$ for the (time-invariant) set of in-neighbors of v , and $P(v)$ for the (time-dependent) subset of $N(v)$ that are active at time t .

The IM problem works on top of the diffusion model, and can be formally defined as follows: given a directed graph $G = (V, E)$, a diffusion model M , and an integer budget k , select a seed set $S \subseteq V$ of size $|S| \leq k$ to maximize the expected number of nodes activated through the diffusion process initiated by S (Kempe, Kleinberg, and Tardos

2003a). We denote the expected final number of active nodes under model M from seed set S by $\sigma_M(S)$.

2.2 Pressure Threshold Model Definition

The PT model is defined on the same graph structure as the LT model and shares the same node activation conditions. Specifically, let $G = (V, E)$ be a directed graph, where V denotes the set of nodes and $E \subseteq V \times V$ denotes the set of directed edges. Each edge $(u, v) \in E$ is assigned a weight $w_{uv} \in [0, 1]$ such that for each node v , $\sum_{u \in N(v)} w_{uv} \leq 1$, where $N(v)$ denotes the in-neighbors of v . Unless otherwise stated, each weight w_{uv} is initialized with a value $1/\text{in-degree}(v)$. Furthermore, each node $v \in V$ is assigned a threshold $\theta_v \in (0, 1]$, which specifies the minimum cumulative influence required from its incoming neighbors for the node to become active.

The diffusion process unfolds in discrete time steps and begins with an initial seed set $S \subseteq V$, where the nodes in S are assumed to be active at time step $t = 0$. Let $A_t \subseteq V$ denote the set of active nodes at time t , with the initial condition $A_0 = S$. At each subsequent time step, the activation of new nodes is governed by the same rule as the classical Linear Threshold (LT) model: a node $v \in V \setminus A_t$ becomes active at time $t + 1$ if the cumulative influence from its currently active in-neighbors meets or exceeds its threshold θ_v . Formally, the activation condition is given by:

$$\sum_{u \in P(v)} w_{uv} \geq \theta_v,$$

where $P(v) = \{u \in A_t : (u, v) \in E\}$ denotes the set of active parent nodes (or in-neighbors) of v .

While the activation rule mirrors that of the LT model, the Pressure Threshold model introduces a key modification through a two-phase update mechanism. Specifically, each round of the diffusion process is composed of the following phases:

1. **Activation Phase:** All nodes that satisfy the activation condition based on the current edge weights and active neighbor states become active.
2. **Influence Adjustment Phase:** The influence exerted by newly activated nodes on their neighbors is recalibrated based on the amount of influence they received during activation.

The rationale for the influence adjustment phase is to model a kind of ancestral amplification: a node that was heavily influenced by its neighbors becomes a more influential source in turn. A node's outbound influence is amplified only once during the timestep of its activation, which prevents recursive feedback loops that could otherwise occur in denser regions of the network. Consequently, the adjustment phase updates only edges toward inactive neighbors, since active nodes remain permanently activated, reducing redundant computation and improving efficiency. To formalize this, let $v \in V$ be a node that becomes active at time step t . Let I_v denote the total incoming influence received by v at the time of its activation:

$$I_v = \sum_{u \in P(v)} w_{uv}.$$

The PT model introduces a tunable amplification parameter $\alpha \geq 0$, which controls the extent to which this received influence translates into increased outgoing influence. For each newly activated node v and for each of its outgoing neighbors s such that $(v, s) \in E$ and $s \notin A_t$, the influence weight is updated according to:

$$w'_{vs} = \min(1, w_{vs} + \alpha \cdot I_v),$$

where w'_{vs} is the new, adjusted influence weight from v to s . The use of the minimum ensures that the updated weights respect the upper bound of 1, consistent with the range of node thresholds. Because the influence added to each edge is directly proportional to αI_v and bounded by the $\min(1, \cdot)$ constraint, the amplification remains small and localized. The additive form of the amplification scheme reflects the additive nature of the threshold activation function in both the LT and PT models. This design ensures that the model remains consistent with the underlying interpretation of influence aggregation. Like other standard diffusion models, this process continues until no new nodes can be activated and is progressive, meaning nodes may go from inactive to active, but never the other way. Algorithm 1 summarizes the complete PT diffusion procedure.

Conceptually, α serves as a reinforcement coefficient that encodes how strongly social feedback amplifies an individual’s influence on their peers. Small values of α correspond to diffusion processes that behave similarly to the Linear Threshold model, while larger values produce stronger social reinforcement dynamics and faster saturation. Because α modulates the intensity of behavioral feedback rather than the network structure itself, in practice it can be treated as a tunable hyperparameter that reflects the degree of social reinforcement present in a given domain and could be estimated or calibrated from empirical diffusion traces, similar to contagion strength in epidemiological models or persuasion intensity in social influence studies (Czuba et al. 2024; Kalimeris et al. 2018).

2.3 Computational Complexity

Theorem 1. *Influence maximization under the Pressure Threshold (PT) diffusion model (PT-IM) is NP-hard.*

Proof. The classical influence maximization problem under the Linear Threshold (LT) model (LT-IM) is NP-hard (Kempe, Kleinberg, and Tardos 2003a). We reduce LT-IM to PT-IM in polynomial time. Given an LT instance (G, k) , construct the PT instance $(G, k, \alpha = 0)$. When $\alpha = 0$, the PT process is identical to LT because the adjustment phase is inactive. Formally, for every seed set S we have:

$$\sigma_{PT}(S; \alpha = 0) = \sigma_{LT}(S).$$

Thus, an optimal solution for PT-IM with $\alpha = 0$ is an optimal solution for the original LT-IM instance. Thus, any polynomial-time algorithm for PT-IM would yield one for LT-IM, giving a polynomial-time many-one reduction. Therefore, PT-IM is NP-hard. \square

Algorithm 1: Pressure Threshold (PT) Diffusion

Require: Directed graph $G = (V, E)$; weights $w_{uv} \in [0, 1]$; thresholds $\theta_v \in (0, 1]$; seed set S ; amplification $\alpha \geq 0$

```

1:  $t \leftarrow 0$ ;  $A_t \leftarrow S$  ▷ initial active set
2: repeat
3:    $N_t \leftarrow \emptyset$  ▷ newly activated at time  $t$ 
4:   for all  $v \in V \setminus A_t$  do ▷ activation phase
5:      $P_t(v) \leftarrow \{u \in A_t : (u, v) \in E\}$ 
6:      $I_v \leftarrow \sum_{u \in P_t(v)} w_{uv}$ 
7:     if  $I_v \geq \theta_v$  then
8:        $N_t \leftarrow N_t \cup \{v\}$ 
9:     end if
10:  end for
11:  if  $N_t = \emptyset$  then
12:    break ▷ no new activations; diffusion halts
13:  end if
14:  for all  $v \in N_t$  do ▷ influence adjustment phase (one-shot)
15:    for all  $(v, s) \in E$  with  $s \notin A_t$  do ▷ only toward currently inactive neighbors
16:       $w_{vs} \leftarrow \min(1, w_{vs} + \alpha \cdot I_v)$ 
17:    end for
18:  end for
19:   $A_{t+1} \leftarrow A_t \cup N_t$ ;  $t \leftarrow t + 1$ 
20: until false
21: return  $A_t$ 

```

Remark (Decision vs. optimization). The theorem above is stated for the optimization problem (maximizing expected spread). For the decision version (“Does there exist $S \subseteq V$, $|S| \leq k$, with expected spread at least T ?”), the same restriction $\alpha = 0$ yields an identical polynomial-time reduction, implying NP-hardness of the decision problem as well.

Corollary 1 (Inapproximability inherited at $\alpha = 0$). *Under $\alpha = 0$, PT reduces to LT. It is NP-hard to approximate optimal influence for LT within a factor better than $1 - 1/e + \varepsilon$ for any $\varepsilon > 0$ unless $P = NP$ (Kempe, Kleinberg, and Tardos 2003a). Consequently, PT-IM inherits the same inapproximability barrier.*

This computational complexity result highlights the necessity of efficient approximation or heuristic approaches for practical applications.

3 Properties of the Proposed Model

3.1 Model Demonstration

To build intuition for the reinforcement dynamics introduced by PT, we present a compact visualization contrasting PT and LT on a small controlled instance. The objective is not to claim generality from a toy example, but to provide a clear, step-by-step view of how additive amplification upon activation changes subsequent propagation compared with the classical, static-weight LT evolution on the same graph.

To illustrate the dynamics of the Pressure Threshold (PT) model, we present a small-scale example with $\alpha = 0.25$ on a 10-node network. Figures 1 and 2 show the early and later stages of PT diffusion alongside LT on the same graph and seed set.

Both models begin with two identical seeds at $t = 0$. Activated nodes are shown in red; nodes newly activated at the current timestep are outlined with a black border; edges whose weights are amplified during the adjustment phase are highlighted in red. As PT evolves, edges incident to newly activated nodes are amplified according to the rule described in Section 2. Using the same seeds, PT eventually achieves full coverage, whereas LT terminates with only five activated nodes.

In the earliest timesteps, PT and LT behave similarly because the initial weights are identical and no adjustment has yet occurred. Differences emerge once the reinforcement mechanism activates: newly activated nodes increase their outgoing influence, allowing neighbors that would remain inactive under LT to cross their thresholds under PT. These incremental adjustments can accumulate in denser regions of the graph and ultimately produce different activation patterns and final reach.

3.2 Monotonicity

We now formalize a basic property of PT that mirrors a key feature of LT. At a high level, adding more seeds cannot reduce the final active set: additional seeds can only help more nodes reach their thresholds, and the adjustment mechanism in PT is applied only when nodes newly activate (never deactivating anyone).

For a seed set S , let $\mathcal{A}(S)$ denote the (random) final active set under PT, and let $\sigma(S) \triangleq \mathbb{E}[|\mathcal{A}(S)|]$ denote the expected spread. We first show a pathwise set inclusion, which implies monotonicity of σ . For any $A \subseteq B \subseteq V$, the following holds for every realization of thresholds and tie-breaking:

$$\mathcal{A}(A) \subseteq \mathcal{A}(B).$$

Theorem 2 (Monotonicity of PT). *For any graph $G = (V, E)$ and seed sets $A \subseteq B \subseteq V$, the PT diffusion satisfies $\mathcal{A}(A) \subseteq \mathcal{A}(B)$ for every realization of thresholds and tie-breaking. Consequently, the expected spread $\sigma(S) = \mathbb{E}[|\mathcal{A}(S)|]$ is a monotone set function.*

Proof. Couple the two processes by using the *same* threshold draws for all nodes. At time 0, all nodes in A are active in both processes, and all nodes in $B \setminus A$ are additionally active in the process started from B . Proceed by induction on time: at each step, a node activates if the sum of incoming weights from currently active in-neighbors is at least its threshold. Since the process from B has a superset of active nodes, any node that activates at a given time under A will also activate (no later than) at the same time under B . The PT adjustment step only *increases* outgoing weights of newly activated nodes; thus it preserves the inclusion. Therefore $\mathcal{A}(A) \subseteq \mathcal{A}(B)$ holds pathwise, and taking expectations gives $\sigma(A) \leq \sigma(B)$. \square

Remark. The argument is a standard coupling: the inclusion on active sets is preserved because PT is progressive (no deactivation) and its weight adjustments are nonnegative and local to newly activated nodes.

3.3 Submodularity Analysis

The LT model is known to produce a submodular influence function (Kempe, Kleinberg, and Tardos 2003b), but the PT model introduces activation-triggered amplification that can violate diminishing returns.

We provide a counterexample showing that $\sigma(S)$ under PT is not, in general, submodular when $\alpha > 0$. A set function f is submodular if for all $S \subseteq T \subseteq V$ and $v \notin T$:

$$f(S \cup \{v\}) - f(S) \geq f(T \cup \{v\}) - f(T).$$

Proposition 1 (PT is not submodular in general). *There exist graphs G , thresholds, and $\alpha > 0$ such that the expected spread $\sigma(\cdot)$ under PT is not submodular.*

Proof. Consider $G = (V, E)$ with $V = \{a, b, c, d\}$ and edges $a \rightarrow c$ with $w_{ac} = 0.4$, $b \rightarrow c$ with $w_{bc} = 0.4$, and $c \rightarrow d$ with $w_{cd} = 0.3$. Let $\theta_c = 0.8$, $\theta_d = 0.4$, $\alpha = 1.0$, $S = \{a\}$, $T = \{a, b\}$, and $v = c$.

Evaluating influence spread:

- $\sigma(S) = 1$: only a is active; c receives 0.4 and stays inactive.
- $\sigma(S \cup \{c\}) = 2$: c is seeded; no amplification occurs when a node is seeded. d receives 0.3 and stays inactive.
- $\sigma(T) = 4$: c receives 0.8 and activates. PT amplifies edge (c, d) to $w'_{cd} = 1$, so d activates as well.
- $\sigma(T \cup \{c\}) = 3$: c is seeded (no amplification); d receives 0.3 and stays inactive.

Marginal gains:

$$\sigma(S \cup \{c\}) - \sigma(S) = 2 - 1 = 1$$

$$\sigma(T \cup \{c\}) - \sigma(T) = 3 - 4 = -1$$

Since $1 > -1$, the submodularity inequality fails, proving the claim. \square

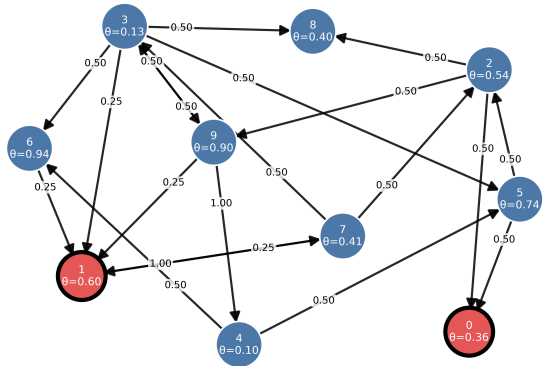
Remark. Due to this non-submodularity, the classical $(1 - 1/e)$ guarantee for greedy (Nemhauser, Wolsey, and Fisher 1978) IM does not generally apply to PT. However, we can reason about approximate submodularity via the submodularity ratio $\gamma_{U,k}(\sigma)$ (Das and Kempe 2018) defined as:

$$\gamma_{U,k}(\sigma) = \min_{L \subseteq U, S: |S| \leq k, S \cap L = \emptyset} \frac{\sum_{x \in S} (\sigma(L \cup \{x\}) - \sigma(L))}{\sigma(L \cup S) - \sigma(L)},$$

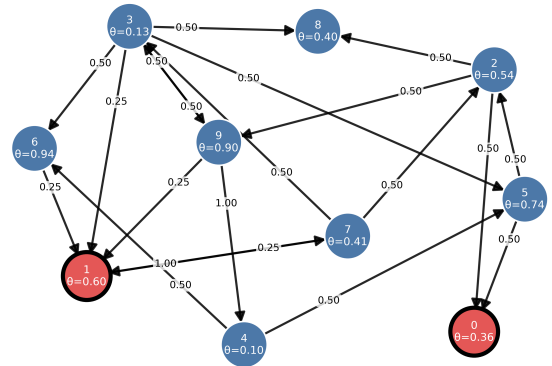
under which greedy achieves a $(1 - e^{-\gamma_{U,k}})$ approximation for the cardinality constraint. Note $\gamma_{U,k} = 1$ means submodularity. In PT, the submodularity ratio $\gamma_{U,k}(\sigma_{\text{PT}})$ satisfies:

$$\gamma_{U,k}(\sigma_{\text{PT}}) \geq \underline{\gamma}(G, \alpha) \quad \text{with} \quad \underline{\gamma}(G, \alpha) \xrightarrow{\alpha \rightarrow 0} 1,$$

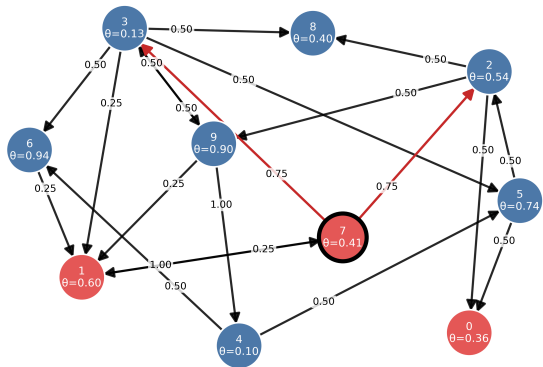
recovering the LT limit and the classical $(1 - 1/e)$ factor. A precise, data-dependent characterization of $\underline{\gamma}(G, \alpha)$ as a function of the graph and pressure is left for future work.



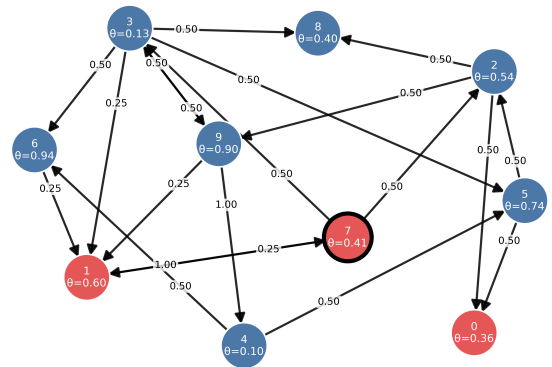
PT Step 0 (No. of activated nodes = 2)



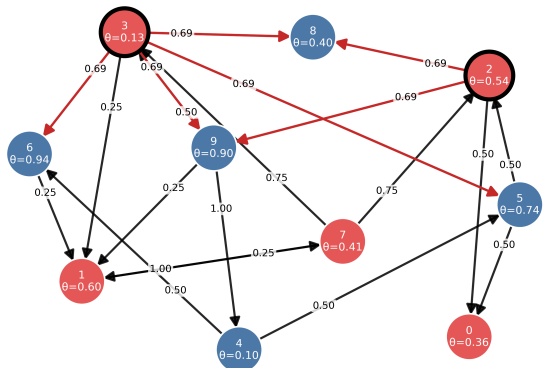
LT Step 0 (No. of activated nodes = 2)



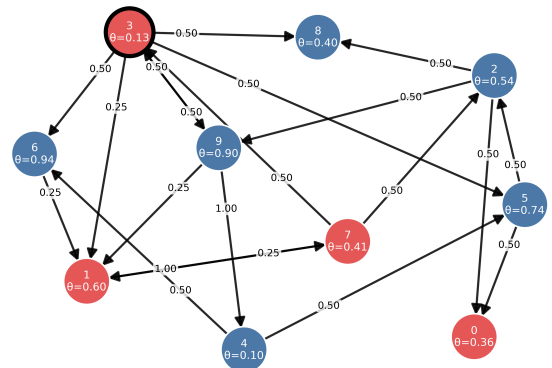
PT Step 1 (No. of activated nodes = 3)



LT Step 1 (No. of activated nodes = 3)

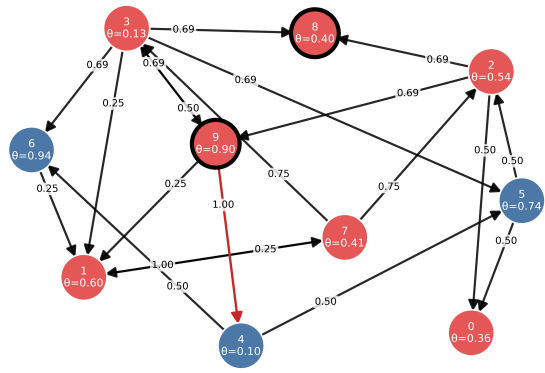


PT Step 2 (No. of activated nodes = 5)

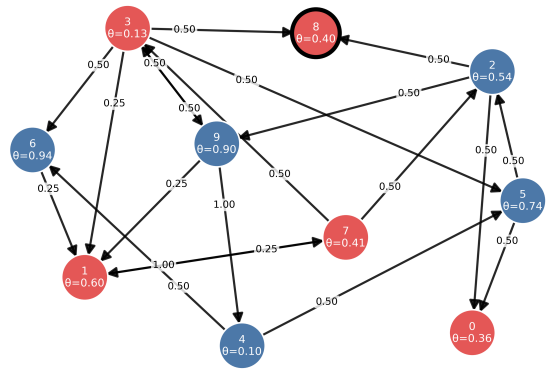


LT Step 2 (No. of activated nodes = 4)

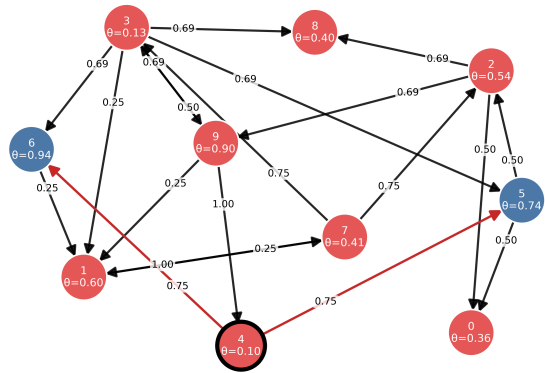
Figure 1: Early diffusion stages under PT and LT on the same graph and seed set. Activated nodes are shown in red, newly activated nodes are outlined in black, and amplified edges are highlighted in red.



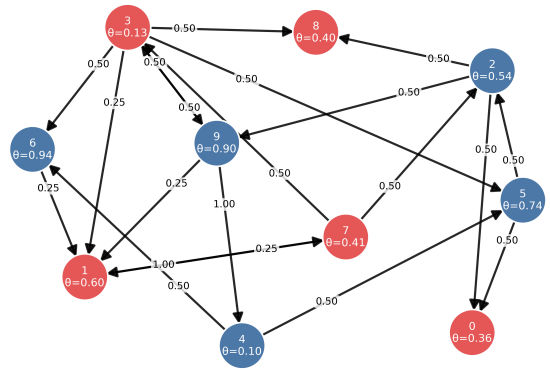
PT Step 3 (No. of activated nodes = 7)



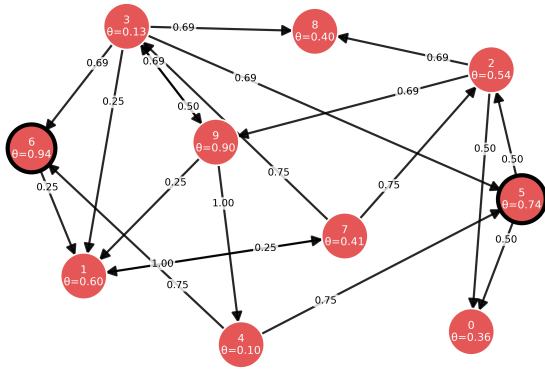
LT Step 3 (No. of activated nodes = 5)



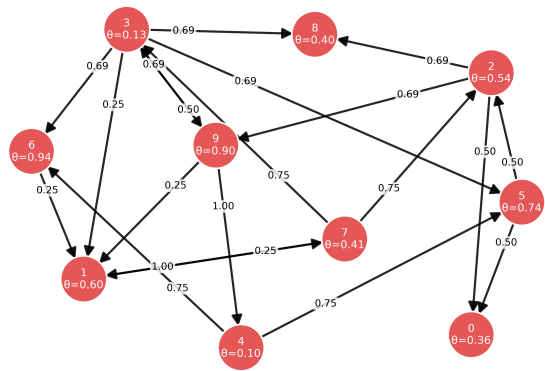
PT Step 4 (No. of activated nodes = 8)



LT Final Step (No. of activated nodes = 5)



PT Step 5 (No. of activated nodes = 10)



PT Final Step (No. of activated nodes = 10)

Figure 2: Later diffusion stages under PT and LT. PT keeps on amplifying edges and attains full coverage, while LT halts sooner.

4 Experiments

4.1 Network Data

We evaluate the Pressure Threshold (PT) model against the Linear Threshold (LT) model on four networks spanning distinct topologies and semantics. Three of these networks are real-world graphs obtained from the Stanford Large Network Dataset Collection (SNAP) (Leskovec and Krevl 2014): (i) Facebook social circles (Leskovec and Mcauley 2012), (ii) Wikipedia voting (Leskovec, Huttenlocher, and Kleinberg 2010a,b), and (iii) Bitcoin OTC trust (Kumar et al. 2016, 2018). To complement these with a purely synthetic baseline, we also include (iv) an Erdős–Rényi random graph $G(n, p)$ (Erdős and Rényi 1959). The number of nodes, number of directed edges, and edge-to-node ratios are reported in Table 1. Throughout, we study progressive cascades (nodes, once activated, remain active) and keep the underlying graph structure fixed during each diffusion run.

Network	Nodes	Edges	Edge/Node Ratio
Facebook	4,039	88,234	21.846
Bitcoin	5,881	35,592	6.052
Wikipedia	7,115	103,689	14.573
Erdős–Rényi	5,000	62,597	12.519

Table 1: Basic statistics of the networks used in experiments.

Graph construction and directionality. The Facebook circles dataset is originally undirected, with an edge indicating a mutual friendship relation. Following standard practice in LT-based diffusion studies (Kempe, Kleinberg, and Tardos 2003b), we convert each undirected edge $\{u, v\}$ into two directed edges (u, v) and (v, u) to preserve symmetric influence opportunities. The Bitcoin OTC trust network is inherently directed: an edge (u, v) represents a rating or trust assignment from user u to user v on a peer-to-peer trading platform. The Wikipedia voting network is also directed: an edge (u, v) indicates that user u voted for user v in an admin election, producing a directed endorsement flow aligned with influence propagation. Similar to the Facebook network, for the Erdős–Rényi random graph, we generate $G(n, p)$ with $n = 5,000$ and $p = 0.005$, and convert each undirected edge into two directed arcs.

Edge weights (weighted-cascade normalization). Unless stated otherwise, we use the weighted-cascade convention (Kempe, Kleinberg, and Tardos 2003b), assigning for each directed edge (u, v) the weight:

$$w_{uv} = \frac{1}{\text{in-degree}(v)}.$$

This ensures that for every node v , the incoming weights sum to one, i.e., $\sum_{u \in N(v)} w_{uv} = 1$. In the PT model, these weights may be updated according to the additive adjustment rule upon activation events (Section 2), while respecting the upper bound $w'_{uv} \leq 1$ via the $\min(1, \cdot)$ cap.

Thresholds and randomness. In all runs, node thresholds θ_v are drawn i.i.d. uniformly from $(0, 1]$ at the beginning of each Monte Carlo (MC) simulation, consistent with the LT literature. For paired comparisons (PT vs. LT) under the same seed budget k , we reuse the same threshold instantiation to isolate model effects from sampling noise. All reported spreads are averages over independent MC trials, with the number of trials specified per experiment.

4.2 Experiment Details

We perform three complementary experiments to probe (i) the qualitative effect of PT’s reinforcement on seed selection (Experiment 1), (ii) the quantitative impact on influence spread versus budget across heterogeneous graphs (Experiment 2), and (iii) the sensitivity of PT to the reinforcement parameter α (Experiment 3). We use the CELF algorithm (Leskovec et al. 2007b) for seed selection in Experiments 1 and 2 to maintain consistency with standard IM practice.

Experiment 1: Seed selection under PT vs. LT. The goal of this experiment is to examine whether PT and LT identify the same influential nodes when given the same budget k . We run CELF on the Facebook network with budget $k = 20$. To evaluate the marginal gains within CELF, we estimate spreads via 1,000 MC simulations per evaluation. For the PT runs we set $\alpha = 0.1$, which empirically balances (i) observable reinforcement leading to altered seed rankings and (ii) avoidance of near-instant saturation. For fairness, the same set of random threshold instantiations is shared between LT and PT whenever possible, ensuring that any observed differences are attributable to the model and not to randomness. The order of seed node selection is preserved for side-by-side comparison.

Experiment 2: Average influence spread vs. budget. To quantify the downstream effect of PT’s reinforcement, we compute the average influence spread $\sigma(S)$ as a function of the seed budget k across the four graphs in Table 1. For each network and each budget $k \in \{1, 2, \dots, 60\}$, we run CELF under three diffusion settings: LT, PT with $\alpha = 0.001$, and PT with $\alpha = 0.005$. Each evaluation of $\sigma(S)$ within CELF averages 1,000 MC simulations. These α values were selected empirically to illustrate qualitative differences between PT and LT while ensuring stable and interpretable diffusion dynamics. Pilot tests with larger α rapidly saturated the denser graphs (Facebook, Wikipedia), while substantially smaller α yielded behavior nearly identical to LT.

Robustness. We additionally tested Normal(0.5, 0.1), Beta(2, 5), and Beta(5, 2) threshold priors; all produced PT–LT spread gaps similar to the uniform prior, so redundant plots are omitted.

Experiment 3: Sensitivity of PT to α . We probe how PT’s final spread scales with the reinforcement parameter by fixing a seed set size ($k = 10$) on Facebook and sweeping α over a fine grid $[10^{-4}, 10^{-1}]$ with step 10^{-4} . For each α , we perform 1,000 MC simulations and report the average spread. To reduce high-frequency variability due to stochastic thresholds, we apply a centered moving average with a

window of 9 grid points; each plotted value is the average of the focal α and its four nearest neighbors.

4.3 Results

The results for Experiment 1 appear in Table 2 and Figure 3. The results for Experiment 2 are shown in Figures 5, 4, 7, and 6. The results for Experiment 3 are given in Figure 8.

Model	Seeds selected (in order)
Linear Threshold	107, 351, 1821, 352, 0, 348, 1831, 349, 366, 1490, 1373, 1827, 2154, 1285, 838, 2806, 1149, 2130, 2403, 2088
Pressure Threshold	107, 351, 352, 1821, 0, 348, 1490, 1215, 1831, 1285, 1426, 1373, 2806, 366, 2403, 3234, 349, 2145, 1827, 2832

Table 2: Ordered seed sets returned by CELF on Facebook with $k = 20$. The overlap in early positions and divergence in later positions reveal how PT’s reinforcement can elevate otherwise secondary vertices.

4.4 Discussion

Figure 3 compares the seed sets that CELF selected under the LT and PT models for a budget of $k = 20$ on the Facebook network. The first column lists the LT seeds, whereas the second lists the PT seeds. Lines connect the vertices common to both seed sets. This graph shows that solving the IM problem under the PT model results in a different answer than under the LT model, providing a key distinction of the former to separate itself from the latter. The models agree on most early selections (those with the largest marginal gains), but diverge more and more in ordering and in selection as the iteration proceeds. From step 8 onward, PT introduces vertices (e.g., 1215) that never appear in the LT list, indicating that amplification can elevate otherwise secondary nodes. Conversely, several LT-specific vertices never surface under PT. Because PT applies an additive effect to edge weights rather than a diminishing one, these omissions imply that other vertices experience larger marginal-gain increases and overtake them in priority. We also observe that the PT model’s seed selection tends to favor nodes embedded within denser regions of the network, where local clustering and mutual reinforcement create more opportunities for amplification compared to nodes with large but sparsely connected neighborhoods. This behavior arises because the PT process implicitly places greater value on a node’s in-degree, reflecting the cumulative pressure it can receive from active neighbors rather than solely on out-degree as in traditional LT and IC models. Table 2 presents the ordered lists in compact form.

Figures 5, 4, 7, and 6 give the average influence of diffusions across the four networks as the budget varies. As expected, network diffusions with the PT model result in a larger average influence spread than the LT model. What is interesting about this experiment is the margin of variation

under the PT model between the different network types. For example, the Facebook and Wikipedia networks result in much larger influence spreads for the PT model than the LT model when compared to the Bitcoin network, whose average influence under the PT model is not much larger than under the LT model. This is most likely due to the larger edge-to-node ratios of the former, as given in Table 1. Intuitively, this makes sense, as more edges yield more opportunity for the influence amplification to take place (phase 2 in the PT diffusion). The amplification was so large that some networks were fully diffused before reaching the max budget of $k = 60$, such as the Erdős–Rényi graph reaching full coverage at $k = 22$. Despite these scale differences, the influence curves for LT and PT maintain similar shapes, suggesting that PT adds an approximately constant offset to the baseline diffusion rate. The logarithmic shape of the PT curves, which matches the diminishing returns of the LT curve, also suggests practical submodularity of the influence spread function on the datasets tested.

Figure 8 shows the average influence spread of a PT diffusion on the Facebook network as a function of the parameter α . Because of the large amount of data points, we applied a centered moving average with a window size of 9 to smooth the α -vs-influence curve. In the graph, each point is replaced by the average of the point itself and the four points to its right and left. As expected, increasing the α value increases the influence amplification at each node, which increases the total influence spread. The fit can be approximated with the following cubic polynomial function:

$$\begin{aligned} \text{Influence}(\alpha) \approx & 1.358 \times 10^6 \alpha^3 - 6.255 \times 10^5 \alpha^2 \\ & + 8.485 \times 10^4 \alpha + 57.29. \end{aligned}$$

5 Conclusion

5.1 Summary of Contributions

In this work, we introduced the Pressure Threshold (PT) model, a diffusion framework that captures reinforcement effects and cumulative influence in social networks. PT extends the Linear Threshold (LT) model by amplifying a node’s outgoing influence according to the pressure it receives from neighbors. We showed that influence maximization under PT remains NP-hard and that PT is monotone but not submodular when $\alpha > 0$, implying that classical greedy guarantees may not fully apply. Experiments on real and synthetic networks demonstrated that PT yields seed sets and spreads distinct from LT, with stronger gains in denser graphs and more modest effects in sparse ones. These findings highlight PT’s ability to model reinforcement-driven diffusion not captured by LT or IC.

5.2 Real-World Implications

The Pressure Threshold model has notable implications for applications such as viral marketing, political campaigning, and information dissemination. By capturing reinforcement phenomena like echo chambers and social amplification, PT can improve predictions of influence spread and help organizations select influential seed nodes more effectively. Consequently, it can inform policymaking for combating misin-

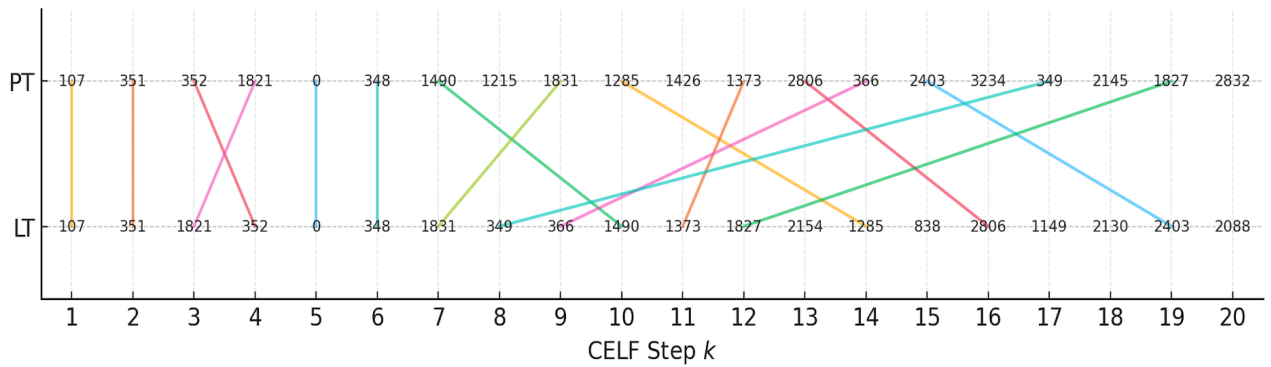


Figure 3: Timeline of seed-node selection by the CELF algorithm on the Facebook network: PT vs. LT ($k = 20$). Horizontal alignment indicates step index; vertical lines connect common seeds appearing in both lists. Early steps overlap strongly; later steps diverge as PT prioritizes nodes positioned to benefit from reinforcement.

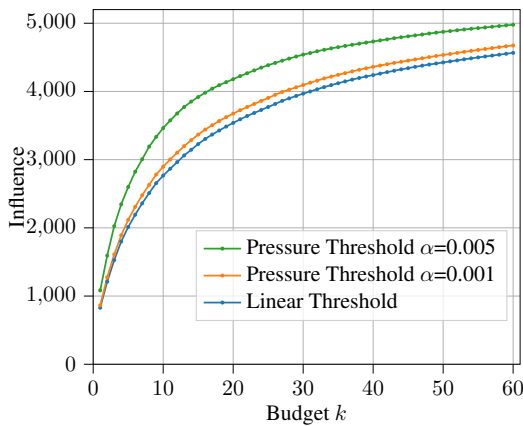


Figure 4: Bitcoin Network: average influence vs. budget. PT’s advantage is present but smaller due to network sparsity and lower local clustering.

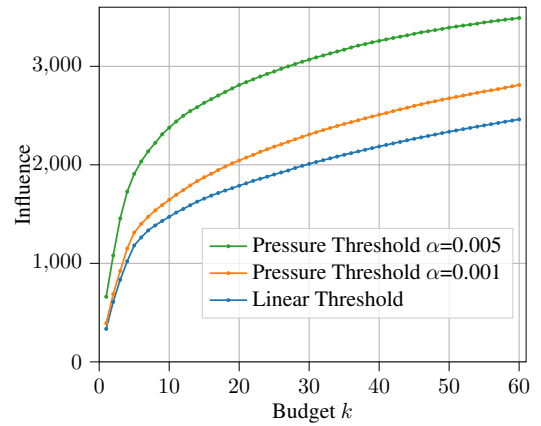


Figure 5: Facebook Network: average influence vs. budget. PT curves exceed LT across budgets; the effect is more pronounced for higher α .

formation and optimizing public awareness campaigns, offering decision-makers a clearer understanding of how local network pressures shape overall influence dynamics.

5.3 Future Work

Future research aims to explore several avenues. First, develop PT-specific approximation methods with guarantees for greedy. In particular, analyze PT via approximate (weak) submodularity—using the submodularity ratio $\gamma_{U,k}$ to obtain data-dependent $(1 - e^{-\gamma_{U,k}})$ bounds that degrade with α and recover LT as $\alpha \rightarrow 0$. Second, conduct predictive validation on large time-stamped cascades and study PT across diverse network topologies and content types. Third, estimate α from empirical traces to reflect domain-specific reinforcement strength. Lastly, extend PT to topic-aware, temporal, and adaptive networks to better mirror real platforms.

5.4 Ethical Considerations

While the PT model offers a useful framework for understanding and optimizing information diffusion, such meth-

ods can also be applied to influence operations or targeted persuasion. We recognize the dual-use nature of diffusion and influence maximization research and emphasize adherence to transparency, accountability, and fairness. When deployed in public communication or policy contexts, amplification and seed-selection mechanisms should be audited to prevent manipulative or discriminatory outcomes. All data used in this study are public and anonymized; no personally identifiable information was processed.

References

- Agarwal, M.; Aggarwal, V.; Umrawal, A. K.; and Quinn, C. J. 2022. Stochastic Top K-Subset Bandits with Linear Space and Non-Linear Feedback with Applications to Social Influence Maximization. *ACM/IMS Trans. on Data Science (TDS)*, 2(4): 1–39.
- Ananthasubramaniam, A.; Zhu, Y.; Jurgens, D.; and Romero, D. 2024. The Role of Network and Identity in the Diffusion of Hashtags. *ArXiv*, abs/2407.12771.
- Aral, S.; and Walker, D. 2012. Identifying Influential

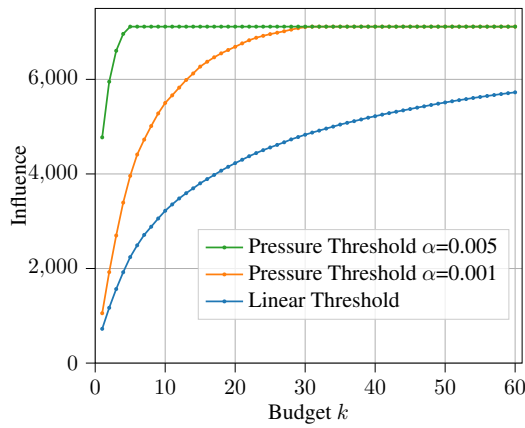


Figure 6: Wikipedia Network: average influence vs. budget. As with Facebook, PT exhibits a clear vertical lift over LT, consistent with more opportunities for reinforcement.

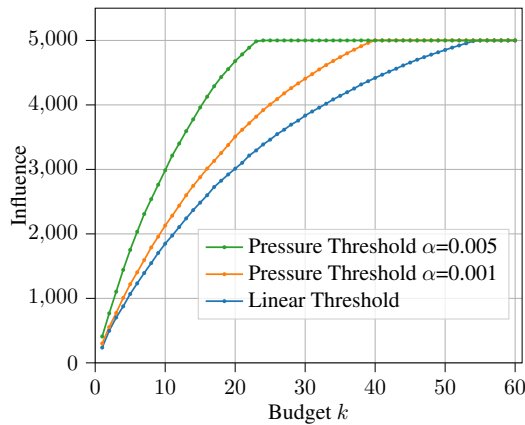


Figure 7: Random Network: average influence vs. budget. Amplification yields rapid approach to full coverage at moderate budgets.

and Susceptible Members of Social Networks. *Science*, 337(6092): 337–341.

Bakshy, E.; Messing, S.; and Adamic, L. 2015. Political science. Exposure to ideologically diverse news and opinion on Facebook. *Science (New York, N.Y.)*, 348.

Becker, R.; D’Angelo, G.; Ghobadi, S.; and Gilbert, H. 2022. Fairness in Influence Maximization through Randomization. *J. Artif. Intell. Res.*, 73: 1251–1283.

Bhimaraju, A.; Robson, E. W.; Varshney, L. R.; and Umrawal, A. K. 2024. Fractional Budget Allocation for Influence Maximization under General Marketing Strategies. In *Procs. 33rd ACM Int. Conf. Inf. Knowledge Management*, 3627–3631.

Borgs, C.; Brautbar, M.; Chayes, J.; and Lucier, B. 2014. Maximizing social influence in nearly optimal time. In *Proceedings of the Twenty-Fifth Annual ACM-SIAM Symposium on Discrete Algorithms*, 946–957.

Brugnoli, E.; Cinelli, M.; Quattrociocchi, W.; and Scala, A.

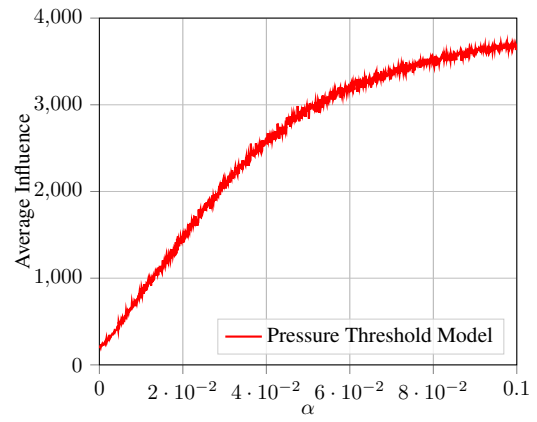


Figure 8: Effect of α on PT spread (Facebook, $k = 10$). The centered moving average (window 9) reveals the monotone increase of final spread with reinforcement strength.

2019. Recursive Patterns in Online Echo Chambers. *Scientific Reports*, 9: 20118.

Chen, W.; Wang, Y.; and Yang, S. 2009. Efficient influence maximization in social networks. In *Proceedings of the 15th ACM SIGKDD International Conference on Knowledge Discovery and Data Mining*, 199–208. Association for Computing Machinery. ISBN 9781605584959.

Chen, W.; Wu, R.; and Yu, Z. 2020. Scalable lattice influence maximization. *IEEE Trans. Comp. Soc. Sys.*, 7(4): 956–970.

Cinelli, M.; De Francisci Morales, G.; Galeazzi, A.; Quattrociocchi, W.; and Starnini, M. 2021. The Echo Chamber Effect on Social Media. *Proceedings of the National Academy of Sciences*, 118(9): e2023301118.

Czuba, M.; Nurek, M.; Serwata, D.; Qiu, Y.-X.; Jia, M.; Musial, K.; Michalski, R.; and Bródka, P. 2024. Network Diffusion Framework to Simulate Spreading Processes in Complex Networks. *Big Data Mining and Analytics*, 7(3): 637–654.

Das, A.; and Kempe, D. 2018. Approximate submodularity and its applications: subset selection, sparse approximation and dictionary selection. 19(1): 74–107.

Domingos, P.; and Richardson, M. 2001. Mining the network value of customers. In *Proceedings of the Seventh ACM SIGKDD International Conference on Knowledge Discovery and Data Mining*, 57–66. ISBN 158113391X.

Erdős, P.; and Rényi, A. 1959. On random graphs I. *Publ. math. debrecen*, 6(290-297): 18.

Evans, D.; and McKee, J. 2010. *Social Media Marketing: The Next Generation of Business Engagement*. John Wiley & Sons.

Goyal, A.; Lu, W.; and Lakshmanan, L. V. 2011. CELF++: optimizing the greedy algorithm for influence maximization in social networks. WWW ’11, 47–48. Association for Computing Machinery. ISBN 9781450306379.

Granovetter, M. 1978. Threshold models of collective behavior. *American journal of sociology*, 83(6): 1420–1443.

- Gunawan, C. M.; Rahmania, L.; and Kenang, I. H. 2023. THE INFLUENCE OF SOCIAL INFLUENCE AND PEER INFLUENCE ON INTENTION TO PURCHASE IN E-COMMERCE. *Review of Management and Entrepreneurship*, 7(1): 61–84.
- Kalimeris, D.; Singer, Y.; Subbian, K.; and Weinsberg, U. 2018. Learning Diffusion using Hyperparameters. In Dy, J.; and Krause, A., eds., *Proceedings of the 35th International Conference on Machine Learning*, volume 80 of *Proceedings of Machine Learning Research*, 2420–2428. PMLR.
- Kempe, D.; Kleinberg, J.; and Tardos, E. 2003a. Maximizing the spread of influence through a social network. In *Proceedings of the Ninth ACM SIGKDD International Conference on Knowledge Discovery and Data Mining*, 137–146.
- Kempe, D.; Kleinberg, J.; and Tardos, É. 2003b. Maximizing the spread of influence through a social network. In *Proc. 9th ACM SIGKDD Int. Conf. on Know. Disc. and Data Mining*, 137–146. ACM.
- Kermack, W. O.; and McKendrick, A. G. 1927. A Contribution to the Mathematical Theory of Epidemics. *Proceedings of the Royal Society of London. Series A, Containing Papers of a Mathematical and Physical Character*, 115(772): 700–721.
- Kumar, S.; Hooi, B.; Makhija, D.; Kumar, M.; Faloutsos, C.; and Subrahmanian, V. 2018. Rev2: Fraudulent user prediction in rating platforms. In *Proc. Eleventh ACM Int. Conf. on Web Search and Data Mining*, 333–341. ACM.
- Kumar, S.; Mallik, A.; Khetarpal, A.; and Panda, B. 2022. Influence maximization in social networks using graph embedding and graph neural network. *Information Sciences*, 607: 1617–1636.
- Kumar, S.; Spezzano, F.; Subrahmanian, V.; and Faloutsos, C. 2016. Edge weight prediction in weighted signed networks. In *Data Mining (ICDM), 2016 IEEE 16th Int. Conf. on*, 221–230. IEEE.
- Kuo, T.-T.; Hung, S.-C.; Lin, W.-S.; de Lin, S.; Peng, T.-C.; and Shih, C. C. 2011. Assessing the Quality of Diffusion Models Using Real-World Social Network Data. *2011 International Conference on Technologies and Applications of Artificial Intelligence*, 200–205.
- Leskovec, J.; Huttenlocher, D.; and Kleinberg, J. 2010a. Predicting positive and negative links in online social networks. In *Proc. 19th Int. Conf. WWW*, 641–650.
- Leskovec, J.; Huttenlocher, D.; and Kleinberg, J. 2010b. Signed networks in social media. In *Proc. SIGCHI Conf. on Human Factors in Computing Systems*, 1361–1370.
- Leskovec, J.; Krause, A.; Guestrin, C.; Faloutsos, C.; VanBriesen, J.; and Glance, N. 2007a. Cost-effective outbreak detection in networks. 420–429. Association for Computing Machinery. ISBN 9781595936097.
- Leskovec, J.; Krause, A.; Guestrin, C.; Faloutsos, C.; VanBriesen, J.; and Glance, N. 2007b. Cost-effective outbreak detection in networks. In *Proceedings of the 13th ACM SIGKDD International Conference on Knowledge Discovery and Data Mining*, KDD '07, 420–429. New York, NY, USA: Association for Computing Machinery. ISBN 9781595936097.
- Leskovec, J.; and Krevl, A. 2014. SNAP Datasets: Stanford Large Network Dataset Collection. <http://snap.stanford.edu/data>.
- Leskovec, J.; and McAuley, J. J. 2012. Learning to discover social circles in ego networks. In *Advances in Neural Information Processing Systems*, 539–547.
- Li, Y.; Gao, H.; Gao, Y.; Guo, J.; and Wu, W. 2023. A Survey on Influence Maximization: From an ML-Based Combinatorial Optimization. *ACM Trans. Knowl. Discov. Data*, 17(9): 133:1–133:50.
- Lin, M.; Sun, L.; Yang, R.; Liu, X.; Wang, Y.; Li, D.; Li, W.; and Lu, S. 2023. Fair Influence Maximization in Large-scale Social Networks Based on Attribute-aware Reverse Influence Sampling. *J. Artif. Intell. Res.*, 76: 925–957.
- Mønsted, B.; Sapiezłyński, P.; Ferrara, E.; and Lehmann, S. 2017. Evidence of Complex Contagion of Information in Social Media: An Experiment Using Twitter Bots. *PLOS ONE*, 12(9): e0184148.
- Nemhauser, G. L.; Wolsey, L. A.; and Fisher, M. L. 1978. An analysis of approximations for maximizing submodular set functions—I. *Mathematical programming*, 14(1): 265–294.
- Nguyen, B.-N. T.; Pham, P. N. H.; Le, V.-V.; and Snášel, V. 2022. Influence Maximization under Fairness Budget Distribution in Online Social Networks. *Mathematics*, 10(22).
- Nie, G.; Agarwal, M.; Umrawal, A. K.; Aggarwal, V.; and Quinn, C. J. 2022. An Explore-then-Commit Algorithm for Submodular Maximization Under Full-bandit Feedback. In *The 38th Conf. on Uncertainty in Artificial Intelligence*.
- Robson, E.; Reddy, D.; and Umrawal, A. 2024. CyNet-Diff: A Python Library for Accelerated Implementation of Network Diffusion Models. *Proceedings of the VLDB Endowment*, 17(12): 4409–4412. Publisher Copyright: © 2024, VLDB Endowment. All rights reserved.; 50th International Conference on Very Large Data Bases, VLDB 2024 ; Conference date: 24-08-2024 Through 29-08-2024.
- Umrawal, A. K.; and Aggarwal, V. 2023. Leveraging the Community Structure of a Social Network for Maximizing the Spread of Influence. *ACM SIGMETRICS Performance Eval. Rev.*, 50(4): 17–19.
- Umrawal, A. K.; Aggarwal, V.; and Quinn, C. J. 2023. Fractional Budget Allocation for Influence Maximization. In *Proc. 62nd IEEE Conf. Decision Control (CDC)*, 4327–4332.
- Vosoughi, S.; Roy, D.; and Aral, S. 2018. The Spread of True and False News Online. *Science*, 359(6380): 1146–1151.
- Xie, M.; Yang, Q.; Wang, Q.; Cong, G.; and Melo, G. 2015. DynaDiffuse: A Dynamic Diffusion Model for Continuous Time Constrained Influence Maximization. *Proceedings of the AAAI Conference on Artificial Intelligence*, 29(1).
- Zhuang, H.; Sun, Y.; Tang, J.; Zhang, J.; and Sun, X. 2013. Influence Maximization in Dynamic Social Networks. In *2013 IEEE 13th International Conference on Data Mining*, 1313–1318.